Journal of Membrane Science and Research 6 (2020) 424-432

Journal of Membrane Science & Research

journal homepage: www.msrjournal.com

Research Paper

Effect of Composite Multi-Walled Carbon Nanotube and Zeolitic Imidazolate Framework-8 on the Performance and Fouling of PVDF Membranes

Nurul Hazreen Wanie Hazmo [1], Rosmawati Naim [1,*], Lau Woei Jye [2], Ahmad Fauzi Ismail [2]

[1] *Faculty of Chemical and Process Engineering Technology, College of Engineering Technology, Universiti Malaysia Pahang, Lebuhraya Tun Razak, 26300 Kuantan, Pahang, Malaysia*
[2] *Advanced Membrane Technology Research Centre (AMTEC), School of Chemical and Energy Engineering, Faculty of Engineering, Universiti Teknologi Malaysia, 81130 Malaysia*

Article info

Received 2020-05-28
Revised 2020-09-02
Accepted 2020-09-20
Available online 2020-09-20

Keywords

Nanocomposite membrane
Anti-fouling
Zeolitic imidazole frameworks 8
Multi-walled carbon nanotube (MWCN)

Highlights

- PVDF nanocomposite membranes was successfully fabricated by incorporating ZIF-8 and MWCNT nanoparticles.
- ZIF-8 was successfully synthesized by detection of hexagonal-shaped.
- Nanocomposites particles improved the membrane morphologies and hydrophilicity.
- Pure water flux and filtration performance of modified membranes are higher than pristine membrane.

Graphical abstract

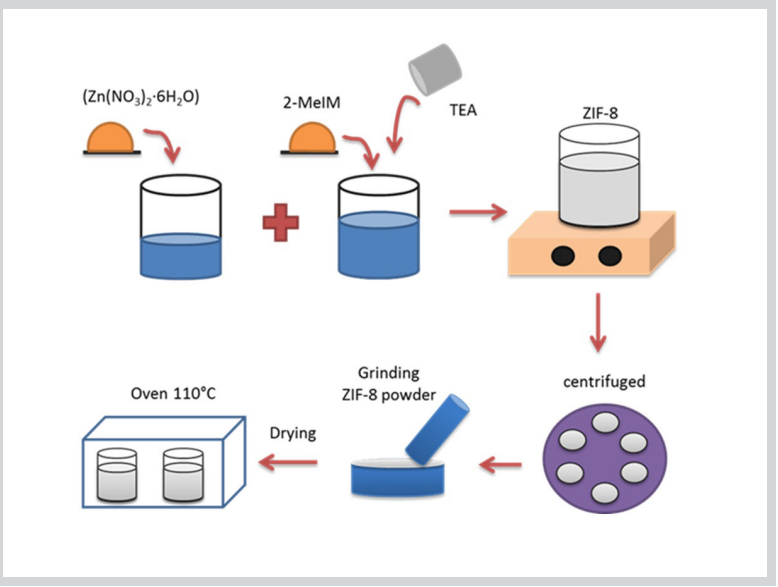

Abstract

The incorporation of nanoparticles into a polymer membrane has been an attractive option to minimize the membrane fouling. Polyvinylidene fluoride (PVDF) nanocomposite membranes incorporated with multi-walled carbon nanotubes (MWCNTs) and zeolitic imidazolate framework-8 (ZIF-8) was prepared in this work via the blending method. The impact of the concentration of inorganic additives (0.1 wt.%, 0.3 wt.% and 0.5 wt.%) on the membrane properties was studied. The prepared membranes were characterized using scanning electron microscopy-energy dispersive X-ray spectrometry (SEM-EDX) and goniometer to investigate changes in membrane properties. Water permeability and filtration performance test were performed using pure water, bovine serum albumin (BSA) and humic acid (HA) solution to evaluate the fouling resistance of the prepared membranes. Even though the permeate fluxes decreased over time, it was found that 0.5 wt.% of ZIF-8 in PVDF membrane produced the highest solute rejection for both HA (>94%) and BSA (>92%) as compared with PVDF/MWCNT membranes and pure PVDF membrane. It is concluded that the nanocomposite membranes showed improvement in the membrane hydrophilicity, permeability, and solute rejection as compared to the pure PVDF membrane. The anti-fouling properties of nanocomposite membranes was enhanced with higher flux recovery rate and lower flux declining rate compared to the pristine PVDF membrane.

1. Introduction

There has been an explosive growth of interest in the development of anti-fouling membranes based on nanoparticles. Membrane fouling is one of the daunting challenges facing by many researchers in membrane separation process. Theoretically, the membrane fouling arises when the membrane surface interacts with the feed water, which contained natural organic matters like humic acid and sodium alginate [1]. Moreover, it was reported that membrane fouling always occurs during the separation process due to the bacterial adhesion, solute adhesion and cake layer formation on the membrane surfaces [2]. These can lead to reduction in the permeate flux and decrease in solute rejection. Therefore, the operation and maintenance cost can be influenced, as well.

The membrane fouling also deteriorates the membrane flux as the foulant adhered to the membrane surface and a thick layer of film (cake layer) is formed and affects the membrane lifespan as well as the membrane

* Corresponding author: rosmawati@ump.edu.my (R. Naim)

DOI: 10.22079/JMSR.2020.128313.1390

performances [3]. In order to overcome this case, it was reported that silver nanoparticles, metal oxide nanoparticles, graphene or graphene-based composites could be employed in membrane separation process since they exhibited high anti-fouling and surface-enhanced properties [4]. The modified membranes have shown an improvement in terms of its morphology, hydrophilicity as well as decrease in the bacterial activity on membrane surface [5]. These two materials (polymer and nanoparticles) interact with one another to form a nanocomposite membrane, which is capable of minimizing the membrane fouling [6].

To date, several carbon-based nanomaterials including carbon nanotubes (CNTs) and zeolites (ZIFs) have been discovered and can be applied in the membrane processess as anti-fouling agents. The incorporation between additives and polymeric material can promote the physicochemical properties of the membrane [7]. Improving the membrane filtration performances through inorganic additive are crucial as failure to address this issue would lead to severe membrane fouling and deteriorate membrane performance over time.

Thus, the incorporation of MWCNTs and ZIF-8 into polyvinylidene fluoride (PVDF) polymer matrix via physical blending method will be discussed further in this study. The composition of the nanoparticles was varied in the range of 0.1– 0.5 wt.% to evaluate the filtration performances of the membrane samples. ZIF-8 nanoparticles were chosen because of its excellent stability, well-defined pore structure and regularity [8]. Meanwhile, MWCNTs show high potential in reducing the membrane fouling due to its hydrophilicity and high surface area [9]. The advantages of MWCNTs are expected to give a huge effects in improving membrane efficiency.

2. Material and methods

2.1. Chemicals

Polyvinylidene fluoride (PVDF) and N, N- dimethylacetamide (DMAc) were purchased from Merck, Malaysia. MWCNTs with >98% carbon, polyvinylpyrrolidone (PVP K-30, MW 30,000Da), zinc nitrate hexahydrate ($Zn(NO_3)_2{\cdot}6H_2O$), triethylamine (TEA), 2-Methylimidazole (2-MeIM) and ZIF-8 were supplied by Sigma-Aldrich. Humic acid and bovine serum albumin were purchased from Thermo Fischer Scientific Inc.

2.2. Synthesization of ZIF-8

ZIF-8 was synthesized according to the procedure described by Nordin et al. [10]. The ZIF-8 nanoparticles were synthesized with a mass ratio of $Zn(NO_3)_2$: 2-MeIM : H_2O in 1 : 6 : 500. For a start, 4 g of zinc nitrate hexahydrate was dissolved in 24.22g of deionized water to produce a metal salt solution. Then, 6.624g of 2-MeIM was weighted and dissolved in 96.90g of deionized water. This mixture was then added 6.0 ml of TEA to produce a ligand solution. Both ligand solution and metal salt solution was then mixed homogeneously for 30 minutes. The solution was placed in a centrifuge machine for 15 minutes and washed with deionized water for complete removal of excess reactants. The product was sent for drying process at temperature of 60°C for 12 hours. Lastly, the product was manually grounded into finer sizes using mortar and pastel before placed into the oven for complete removal of water at 110°C for 12 hours.

2.3. Preparation of flat sheet membrane

Firstly, the PVDF dope solutions with the composition of nanoparticles were prepared as shown in Table 1. The nanocomposite membrane was prepared using PVDF and PVP as the base polymer matrix, DMAc as the solvent, and ZIF-8 and MWCNTs nanoparticles as the inorganic additives.

The preparation of the polymer dope solution was based on procedure described by Dong et. al. [11] where the ZIF-8 loading was determined by the total solids percentage as stated in Equation 1:

$$Filler\ loading\ (\%) = \frac{M_f(g)}{M_s(g)} \times 100\% \quad (1)$$

where $M_f\ (g)$ is a mass of filler in gram while $M_s\ (g)$ is the mass of polymer in gram. First of all, PVDF pellets were weighed and dried in an oven at 60°C and left overnight, while the synthesized ZIF-8 was dried at 100°C for at least 12 hours to remove trapped water. Then, the PVP was weighed and added to the DMAc solution. Different amount of ZIF-8 (see Table 1) was added to DMAc-PVP solvent and sonicated for 2 hours (34°C) to disperse the ZIF-8 solvent uniformly. The PVDF pellets were then added to the ZIF-8 suspension and stirred at uniform speed for 24 hours to obtain homogenous solution. For complete removal of air bubbles, the dope solution was then left overnight at room temperature before the cast. Another dope solution without nano-filler was produced as the control membrane (P0).

After the preparation of polymer solution, fabrication process of the flat sheet membrane was performed. The solution was cast manually on a clean glass plate using a casting bar at ambient atmosphere. The cast film was then immersed in a water bath for removal of excess solvent and completion of phase inversion process. The measured membrane thickness is in the range of 120-190 µm. Then, the membrane was rinsed, labelled and stored in the chiller at 4°C for further use. The same procedures were also used to prepare the control sample (P0).

2.4. Membrane characterization

2.4.1. Physicochemical characterization PVDF membrane

Scanning electron microscopy with an energy dispersive X-ray spectrometer (SEM-EDX Hitachi TM3030Plus, Japan) was used to analyse the PVDF membrane cross sectional structures and its composition. The membrane samples were fractured in liquid nitrogen and sputtered with a fine layer of gold. Wettability of the membrane were investigated by measuring the contact angle of the membrane samples by goniometer. A fine drop of water was placed on the membrane's surface to measure the contact angle. The average value of contact angle was recorded at several position on the membrane surface. The ZIF-8 was characterized using transmission electron microscope (TEM) at 200 kV to verify its properties in term of physical and chemical properties (TECNAI G2 20 Twin).

2.4.2. Pure water flux measurement

The membrane performance was evaluated via pure water permeability flux and solute rejection test. A cross-flow ultrafiltration cell (CF042, STERLITECH) was used with 42 cm^2 membrane surface area and flowrate of 0.2 L/min was applied. Deionized water was used as a feed water for pure water permeability test and a pre-compaction pressure was set at 1.5 bar for 30 minutes before conducting the experiment at room temperature. The operating pressure was maintained at 1.0 bar for 15 minutes to reach a steady state. The permeates was taken every 10 minutes and the permeation flux, J, was calculated by using Equation 2:

$$J_1 = \frac{V}{A \times \Delta t} \quad (2)$$

where V represents the total volume of permeate pure water, A for membrane area and Δt for time interval.

2.4.3. Filtration test

In this work, the solute rejection tests were performed to understand the anti-fouling performance of the membrane samples. Bovine serum albumin (BSA) and humic acid (HA) were used as a standard model of natural organic matters (NOM) in this study. Since HA solute is part of common organic matters found in the surface of water, it has been used to represent the common organic matters in this separation process. Moreover, BSA and HA can be used as well as to estimate the pore size of the membrane samples produced.The procedures and conditions used were similar to the pure water permeability test.

Table 1
Nano-fillers contents in the flat sheet membranes.

No. sample	PVDF (wt.%)	DMAc solution (wt.%)	PVP (wt.%)	ZIF-8 (wt.%)	MWCNT (wt.%)
P0	15.0	84.0	1.0	-	-
Z1	15.0	84.0	1.0	0.1	-
Z2	15.0	84.0	1.0	0.3	-
Z3	15.0	84.0	1.0	0.5	-
M1	15.0	84.0	1.0	-	0.1
M2	15.0	84.0	1.0	-	0.3
M3	15.0	84.0	1.0	-	0.5

The filtration test was carried out for 2 cycles with total of 120 minutes of operational time and the final permeation flux, J_P was recorded. The test was carried out for each membrane. Then, the fouled membrane was rinsed with deionized water for 30 minutes and the flux of cleaned membrane, J_R was measured. The antifouling properties of the membrane can be evaluated through flux recovery ratio (*FRR*), flux decline rate, R_t and the percentage of solute rejection, *R* as calculated using Equation 3, 4, and 5, respectively:

$$FRR = \frac{J_R}{J_0} \times 100\% \quad (3)$$

$$R_t = 1 - \frac{J_R}{J_0} \times 100\% \quad (4)$$

$$R = 1 - \frac{C_P}{C_f} \times 100\% \quad (5)$$

where J_0 is initial flux of each cycle and C_f and C_P are the concentration of feed solution and permeate solution. HACH DR5000UV-Vis Spectrophotometer was used to measure the permeates and feed solution of BSA and HA at a wavelength of 254 nm and 280 nm.

3. Results and discussion

3.1. Characterization of ZIF-8

ZIF-8 nanoparticles were employed in this study as the inorganic additives incorporated into PVDF solution dope to investigate its anti-fouling ability. The ZIF-8 was synthesized and characterized via TEM analysis to confirm their shape and particle sizes before preparing the dope solutions. Figure 1 depicted several images of TEM analysis on synthesized ZIF-8 at various magnifications. From the observation, it was found that the synthesized ZIF-8 produced a well-defined hexagonal structures with particle sizes of 140 to 160 nm. This result was in good agreement with Nordin et al. [10,12] as they reported the size of the particles was around 134 nm. The presence of TEA loadings might slightly affect the particle sizes of the synthesized ZIF-8.

Structural defects was observed on the particles surfaces of synthesized ZIF-8 as shown in red circle in Figure 1(A). Since other parameters such as temperature, method of synthesis, mixing rate, reaction rate and their control were kept constant, these structural defects can be related to the fast crystal formation. The crystals irregularities could be induced by crystal shearing as the solution concentration increased [12]. Therefore, it is reasonable to deduce that the rapid crystal formation resulted from highly concentrated synthesis solution, and the crystal irregularities resulted from the addition of TEA.

3.2. Membrane morphology analysis

Cross-sectional structure of pristine PVDF membrane, PVDF/ZIF-8 and PVDF/MWCNT membranes were depicted in Figure 2. It was observed that the morphologies for all nanocomposite membranes were completely different from the pristine membrane. A more porous and spongy structure was observed for the nanocomposite membrane while the pristine membrane exhibited more compact and denser structure. This was due to the rapid liquid-liquid phase change that occurred as a result of instability of process thermodynamic. This result was further supported by Alpatova et al. [13] in which during the membrane formation, the addition of nano-fillers caused declination of the system thermodynamic stability and led to rapid mass transformation with formation of more porous structures.

Upon addition of zeolite materials, the cross-section morphology of the membranes became more porous than the pristine membrane. It was observed that narrow finger-like structures was produced by Z1, Z2, Z3, and M1 membranes while larger macro-voids was observed for M2 and M3 membranes. This may due to the high diffusion rate of solven-nonsolvent exchange during the fabrication process, which attributed to the larger pore size and more sponge-like structures. Bottino et al. [14] supported this statement as they observed an asymmetric structure with a selective thin microporous layer and finger-like cavities on a hybrid membranes. This could be related to the high mutual diffusivity of solvent and water during the fabrication process of membrane.

In Figure 2, when 0.1 wt% ZIF-8 content was added, nanocomposite membrane revealed larger finger-like structures and the finger-like became narrower and more sponge-like as the concentration of nanoparticle increases. In addition, the SEM results showed that the structure on the top layer of the membranes became more compact when the concentration of ZIF-8 was added to 0.3 wt.% and 0.5 wt.%. The result was in good agreement with Ibrahim et al [15] as they found that the membrane structure was more compact upon addition of 2–8 wt% of ZIF-8 nanoparticles as a result of reduced solvent nonsolvent exchange rate. Taurozzi et al. [16] also reported that the increase in polymer solution viscosity due to the presence of ZIF-8 nanoparticles could slow down the phase separation process, reducing membrane pore size.

From the SEM analysis, it was found that PVDF/MWCNT membranes produced more porous structure compared to other PVDF membranes. A smaller pores were spotted on the upper layer of nanocomposite membranes while larger pores were formed at the bottom layer. This may be due to the mass transformation between solvent and water was alleviated by MWCNTs during the phase inversion process. This is in agreement with Silva et al. [17] in which they found that membranes fabricated with 0.2-0.5 wt% of MWCNT presented the sponger-like pores with increased nanoparticles concentration. The author also concluded that the macrovoids structure formed in the hybrid membranes was influenced by the oxygen functional groups that interacted with the polymer chains.

Additionally, MWCNTs is well-known as one of the hydrophilic materials as they contained high oxygen-functional groups that accelerated the diffusion rate between the solvent and non-solvent during the fabrication process. Therefore, larger pore channels were formed due to the rapid liquid-liquid phase separation process. This could affect the membrane permeability which was observed from the increment in membrane pores size as agreed by Yu et al. [18]. Relatively, as the contents of nanoparticles escalate, membrane pore sizes tend to increase which could be related to increases in membranes permeability of the MWCNTs. It was found that the M3 membrane produced the largest macro-voids which led to high water flux.

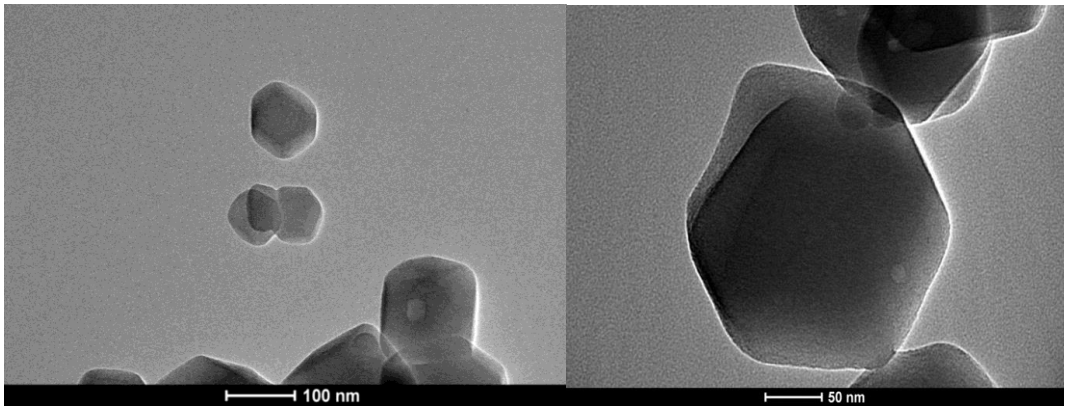

(A) (B)

Fig. 1. Synthesized ZIF-8 images at different magnifications via TEM; (A) scale of 100 nm and (B) scale of 50 nm.

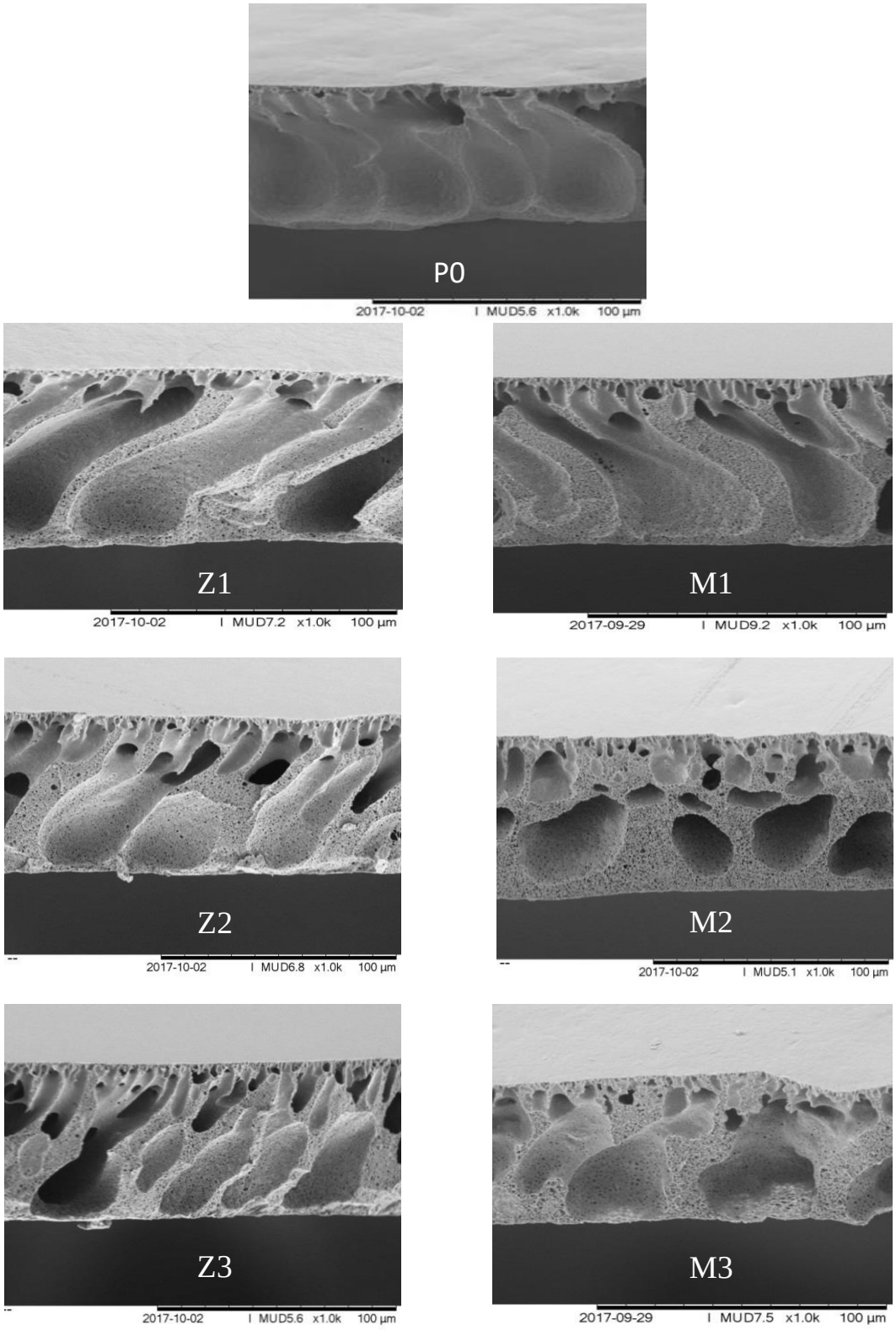

Fig. 2. SEM images of cross section of all membranes; P0 (Pure PVDF); Z1, Z2, Z3 (0.1 wt.%, 0.3 wt.%, 0.5 wt.% ZIF-8); M1, M2, M3 (0.1 wt.%, 0.3 wt.%, 0.5 wt.% MWCNTs).

3.3. Energy dispersive X-ray spectrometry analysis

Table 2 illustrates a quantitative elements which may presented on the surface of PVDF membranes. The presence of main elements such as C and F in the data represented the carbon and fluorine in PVDF polymer. The quantitative analysis of PVDF/ZIF-8 membranes showed the presence of zinc (Zn), confirming the ZIF-8 nanoparticles was successfully embbedded in the nanocomposite membrane. It can be said that the zinc element was fully-distributed on the membrane matrix as proven by the value of Zn loading on the membrane surface. For instance, Z2 membrane sample contains 0.278 wt% of Zn, which in good agreement with the calculated filler loading (using Equation 1) with 0.299 wt.% of Zn loading. This would imply that the ZIF-8 nanoparticles were thoroughly dispersed in the polymer solution during membrane fabrication process. This result was in accordance with Nordin et

al. [10] where they reported that the zinc elements were well scattered throughout their membrane samples.

The new elemental zinc, oxygen and aluminium found in the membrane matrix other than of C and F, were from ZIF-8 and MWCNT, respectively. In this work, MWCNT was mainly consisted of elements C, O, H with > 98% carbon basis. Another 2% of the elements that may be found in the CNT was aluminium (Al) from Al_2O_3 electrode substrate. As indicated in Table 2, the carbon loading increased in accordance to the addition of MWCNT indicating that it has fully dissolved in the polymer matrix and the presence high oxygen element verified the existence of CNTs in the membrane matrix.

3.4. Contact angle analysis

The average contact angle values for PVDF membrane was tabulated in Table 3. The pristine membrane showed a lower contact angle of 77.81° despite of ~85.20° due to addition of 1 wt.% of PVP in the polymer solution, making the membrane more hydrophilic [19]. In comparison, the nanocomposite membranes tend to be more porous and spongier upon addition of nanoparticles concentration, as illustrated in Figure 2.

The results showed an improvement in the membrane hydrophilicity upon the addition of ZIF-8 and MWCNT nanoparticles into the membrane matrix. This can be explained by the incorporation of nano-filler which act as a pore-enhancing agent owing to the hindrance effect to enhance the pore size and porosity of the membrane with the increase in velocity of solvent inter-diffusion, as confirmed by Kim et al. [20]. In addition, the enhanced hydrophilicity was also suggested by the polar characteristic of zinc nanoparticles and polar functional groups of graphene [21].

Results of contact angle values of PVDF membranes showed a decreasing pattern as the concentration of nanoparticles increases. It was observed that the PVDF/ZIF-8 membranes have higher contact angle values compared to PVDF/MWCNT membranes. This trend occurs due to the nature of ZIF-8 which was slightly hydrophobic and caused the nanoparticles to stay at the bottom layer of the membrane. It can be noted that the hydrophilicity of PVDF/ZIF-8 membrane increases with nanoparticles concentration where the recorded contact angle value of membrane Z1 is 66.51°, Z2 (64.41°) and Z3 (58.23°). The result is supported by Aljundi et al. [22] where the increment in ZIF-8 concentration has resulted in decreased contact angles which due to slower solvent-nonsolvent exchange rate.

3.5. Pure water permeability

The water flux of nanocomposite membranes was investigated using an experimental ultrafiltration system at 1 bar. Figure 3 depicted the results of water flux for PVDF membranes. The pure water flux of PVDF/ZIF-8 membranes increased (up to 56.96 L/m^2.h) in comparison with pristine membrane when the content of nanoparticles increases. This showed that a small number of nanoparticles was enough to facilitate the permeation flux by 40%. This is due to the nature of additives used which has improved the hydrophilicity of membrane and increased the water permeation fluxes. As demonstrated in Table 3, the membrane fluxes were in good agreement with contact angle data as the lowest contact angle resulted in the highest water flux. This showed that membrane hydrophilicity played a great role in promoting the water flux. The same trend also reported by Duan et al. [23] when they applied hydrophilic nanoparticles as additives into the polymer matrix. The membrane showed an increase in surface hydrophilicity and water flux when GO was introduced into the membrane structure.

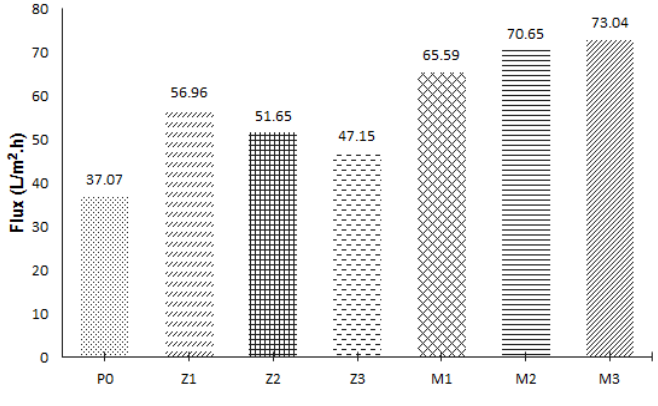

Fig. 3. Pure water flux for all membranes samples at operating pressure (1 bar).

Table 2
EDX quantitative analysis of all membranes.

Sample	C	F	Zn	O	Al
P0	38.636	49.814	-	4.601	-
Z1	40.421	49.004	0.078	5.651	-
Z2	43.790	38.537	0.278	8.105	-
Z3	34.668	52.311	0.963	4.713	-
M1	22.601	26.279	-	6.284	2.389
M2	24.150	16.480	-	7.007	1.334
M3	44.161	43.460	-	7.476	0.066

Table 3
Contact angle of PVDF membranes.

Membrane	Average Values	Standard Deviation
P0	77.81	± 0.61
Z3	66.51	± 1.04
Z2	64.35	± 1.03
Z1	58.23	± 0.90
M1	60.66	± 1.39
M2	56.26	± 0.68
M3	53.59	± 0.71

In addition, the membrane structures played a great impact on the anti-fouling property and filtration performance. From the SEM images (Figure 2), the morphologies of nanocomposite membranes revealed a more porous structure as compared to pristine PVDF membrane. This may be due to increasing in membrane pores which effectively facilitate the passages of water molecules through the membrane. It was reported by Zhao et al. [24] that the blended membranes showed a larger pore and inner structures with addition of MWCNT, which undoubtedly facilitate the pure water flux.

Furthermore, Rahimpor et al. [25] stated that addition of nanoparticles as additives will increase the permeation flux as the presence of fillers enhance the pore channel, whereas high concentration of fillers will reduces the flux due to more compact and thicker skin layer as a result of the slower exchange rate of solvent-nonsolvent during fabrication process. In addition, Xu and Xu [26] reported that the addition of PVP into polymer matrix promoted the membrane morphology as enhanced membrane porosity and hydrophilicity will increase the permeation flux. In comparison with those of pristine PVDF membrane (Figure 2, their hydrophobic nature with dense structure and less macro-voids could contributed to high transport resistance across the membranes thus reducing the water flux.

From the observation in Figure 3, a lower water flux can be observed at higher ZIF-8 nanoparticle loadings, which may be due to pore blockage or agglomeration of nanoparticulates in the membrane matrix. Consequently, adding a higher concentration of nanoparticles caused higher viscosity, which leads to thicker and denser skin layer formation and increases permeability resistance as agreed by Farahani and Vatanpor [27]. Although sonification has been done for fully dispersion of the nanoparticles in the dope solution, agglomeration still occurred at higher concentration of nanoparticles and resulted in decline of water flux. As mentioned in previous EDX analysis, the value of Zn and O contents in the membrane matrix increased rapidly for 0.5 wt.% of ZIF-8 and MWCNT. This showed that agglomeration has occurred due to excess contents of the nanoparticles in the membrane samples. The severe pore blockage also contributed to permeation reduction as previously reported by Rabiee et al. [24].

In addition, it was emphasized that the pure water flux of PVDF/MWCNT membrane increases with increasing nanoparticles concentration in the PVDF membranes. Further increment of nanoparticles resulted in high water flux which may due to more sponge-like and increases in macro-void structures. From the observation in Figure 3, the membrane sample of M3 has the highest water flux of 73.04 L/m^2.h. This may due to the improvement in the permeability of M2 and M3 which enhanced by oxygen-

functional group in MWCNT [28]. According to Meng et al. [29] the hybrid membrane with a more porous surface and favorable inner structures could effectively attribute to a higher permeability of the membrane. Moreover, the hydrophobic nature of the pristine PVDF membrane does not contributeed to membrane water flux. The results shown in Figure 3 proved that the PVDF/MWCNT membranes produced higher permeability as compared to other PVDF membranes.

3.6. Membrane filtration test

BSA and HA solutions were used as the feed to study the membrane filtration performance. The permeation fluxes for BSA and HA solution are presented in Figure 4 and Figure 5. From Figure 4, it was found that the permeate flux of BSA solution for PVDF/ZIF-8 membrane increased significantly compared to the pristine membrane. It was observed that membrane Z3 has higher flux (33.25 L/m^2.h) in comparison with pristine membrane (P0) which was 29.76 L/m^2.h. However, membrane M2 and M3 showed higher flux compared to Z3 membrane. This may due to the differences in more sponge-like and less macro-voids structures produced by M2 and M3 membranes.

Additionally, the simple blending method for preparing the nanocomposite membranes affected the results of the filtration test which lead to a lower permeate rate of PVDF/ZIF-8 membranes compared to PVDF/MWCNT membranes. The possible reason was due to the aggregation and low dispersion of ZIF-8 nanoparticles in PVDF polymer, which was due to clogged pores in the membrane matrix. Longer contact time has resulted in further decrease in permeate fluxes. This phenomenon was due to the pore blockage in the membrane structures that prevented the water to pass through. Eventually, a thick layer of film was formed due to the deposition of solutes onto the membrane surfaces. This is supported by Tang et al. [31] and Arkhangelsky et a.l [32] as they declared that solutes with a smaller size than membrane pores were transported through easily, whereas bigger solutes were rejected. This is due to the pore-clogging inside the membrane structures and reduced the water passages throughout the membrane.

The same trend also applied for the HA solution as shown in Figure 5. It was observed that the membrane sample (Z1, Z2 and Z3) depicted decreasing permeate fluxes within 10 min of operation. It was anticipated that the differences value of molecular weight of humic acid solute (20-500 KDa) have affected the results of flux and solutes rejection. Higher permeate flux of membrane with more porous structures can be achieved due to the smaller solutes in HA solution which can passed through the macro-voids. The membrane samples of M2 and M3 showed higher flux in comparison with other nanocomposite membranes and pristine membranes, while the fluxes kept decreasing as the operational time increases.

Although PVDF/ZIF-8 membranes exhibited denser structures than PVDF/MWCNT membranes, their permeability was higher than the pristine PVDF. This probably was due to the improvement in surface hydrophilicity which control the permeate flux. Higher hydrophilicity allowed the water to pass through the membranes easily. According to Hu et al. [33] higher hydrophilicity was related to the higher adsorption of water molecules in membrane pores with lesser interaction, and thus elevated the permeability. Besides, Marel et al. [34] mentioned that the permeation flux could be greatly affected by surface roughness, hydrophilicity, membrane pores and porosity. Moreover, the enlarged roughness could aid in the increment of filtration area thus enhanced the permeation flux. However, as ZIF-8 content increased, the permeates showed a decline in values. These trends can be explained by the increased viscosity of polymer solution due to the increase of ZIF-8 concentrations. Khan et al. [35] mentioned that higher viscosity of dope solution caused slower mass transformation thus producing a compact membrane structure with smaller pores. However, based on Figure 4 and Figure 5, both BSA and HA fluxes of all nanocomposite membranes were declined during the filtration process. The solute permeation fluxes can be interpreted as membrane fouling, in which the more the curve declined, the more membrane was fouled. A cake layer was formed on the membrane surface after the filtration process, indicating that the membranes have been fouled by the feed water. After in contact with the solutes, a layer of thick film was formed because of solutes deposition on the membrane surfaces and reduced the permeate fluxes. It was proved by Turcaud et al. [36] that the HA depositions on membrane surface caused formation of film layer, which the increase of membrane thickness and declines the HA fluxes. Additionally, although the adsorption reached its capacity, the rejections will decrease gradually as time passed. The flux recovery ratio (*FRR*) and flux decline rate, R_t were employed to determine the anti-fouling properties of the membrane samples and the results are shown in Table 4.

Obviously, the nanocomposite membranes showed an increase in the *FRR* after the cleaning process compared to the pristine membrane. The sample of M3 presented highest flux recovery of BSA solution with 90.98% (1st cycle) and 87.56% (2nd cycle), and highest flux recovery of HA solution with 92.28% (1st cycle) and 89.67% (2nd cycle), indicating the membrane has high anti-fouling resistant. The greater value of flux ratio and lower flux decline rate presented better anti-fouling properties of the nanocomposite membranes as a result of incorporating hydrophilic additives.

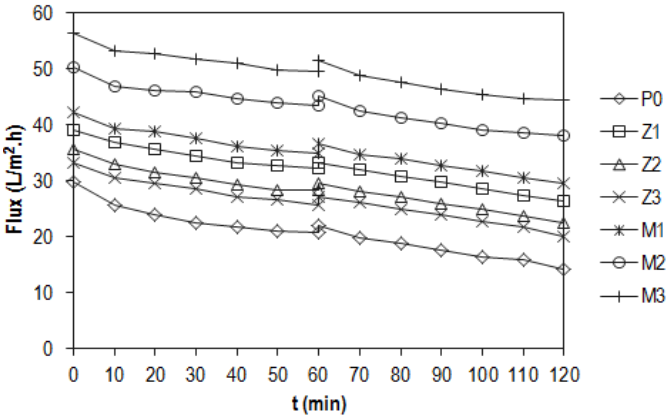

Fig. 4. Permeate fluxes for BSA solution for all membrane samples. Operating pressure = 1bar at room temperature with BSA concentration = 500 ppm.

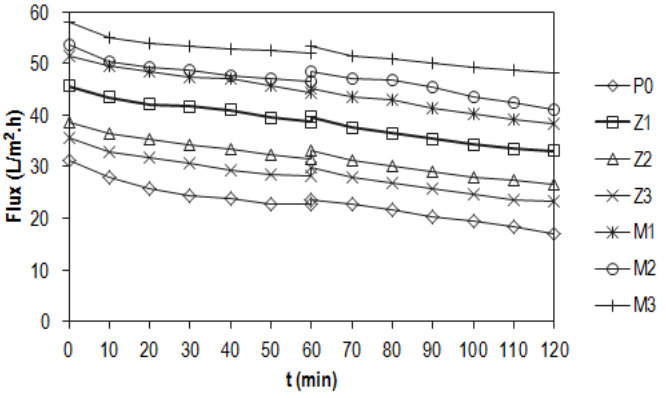

Fig. 5. Results of Permeate Fluxes for HA Solution for all Membrane Samples. Operating Pressure=1bar at room temperature with HA Concentration=500ppm.

Table 4
FRR and R_t for all membrane samples. Operating pressure = 1 bar at room temperature.

Sample	Solute	FRR C1	FRR C2	R_t C1	R_t C2
P0	BSA	73.82	64.86	29.97	35.55
	HA	75.20	68.56	27.45	27.72
Z1	BSA	85.09	81.64	17.90	20.77
	HA	86.87	82.33	15.11	16.63
Z2	BSA	83.26	78.84	20.46	24.20
	HA	85.80	80.65	18.40	19.24
Z3	BSA	81.62	75.47	23.16	26.01
	HA	83.92	77.85	21.13	22.47
M1	BSA	86.85	81.57	17.50	19.50
	HA	87.72	82.72	13.80	15.35
M2	BSA	89.47	85.65	13.94	15.38
	HA	90.21	86.45	13.26	14.94
M3	BSA	90.98	87.56	12.33	13.41
	HA	92.28	89.67	10.20	10.06

Compared to that of P0 membrane, the solute deposition on nanocomposite membrane surfaces was easily removed by membrane rinsing. These results revealed that the nanocomposite membranes possessed higher anti-fouling properties compared to the pristine membranes. According to Hashino et al. [37], the hydrophilic membrane tends to have a higher anti-fouling property as the formation of hydration layer on the membrane surfaces provided higher resistance against solutes depositions and induced pore-clogging, thus weakening the hydrophobic interaction between the solute and membrane surfaces.

However, a significant permeate loss was observed in the sample P0 compared to the nanocomposite membranes. Even after cleaning, the FRR of BSA solution could only return to 73.82 (1st cycle) and 64.86% (2nd cycle) of its initial flux. This result revealed that irreversible fouling has occurred to pristine membrane, which was influenced by its hydrophobic nature. Meanwhile, the nanocomposite membranes showed less permeate loss after addition of nanoparticles and the cleaning process was effectively recovered to it's initial fluxes. This showed that anti-fouling performance of the nanocomposite membranes has been improved significantly. These results could be supported by Zhao et al. [38] whereby the addition of nanoparticles in the membrane matrix has improved the anti-fouling properties of the membrane. This may be associated to the increase in membrane hydrophilicity which has reduced the affinity between the membrane surface and the proteins.

Based on Figure 6, it was noted that the BSA rejection increases as the nanoparticles concentration increased in PVDF membranes. Among the samples, membrane Z3 has the highest BSA rejection compared to other membranes due to its well-formed structures. The improvement in the percentage of BSA rejection can also be influenced by the incorporation of both ZIF-8 and MWCNT into PVDF membranes, as compared to the pristine membrane. Meanwhile, as for PVDF/MWCNT membranes, their slightly thinner layer has caused a lower BSA retention, compared to the ZIF/PVDF membranes.

Greater solute rejection was achieved by sample Z3 as its smaller pores size on the upper layer of the membrane structure caused the PVDF/ZIF-8 membrane became less sensitive to solute deposition. This is due to the smaller pore size that minimized the number of membrane entrance so that solutes cannot enter the pore length easily. This would prevent the phenomenon of pore blockage and pore narrowing that could trigger the membrane fouling in the filtration system. As observed in Figure 6 and Figure 7, the PVDF/ZIF-8 membranes were concluded to have the greatest ability in separating the solutes. The variations in solute rejection of each membrane was in accordance with the improved pore size because of the increased of ZIF-8 concentrations. As of CNTs, it was reported that it has the ability to eliminate albumin as it can also function as an adsorbent [39]. As observed from Figure 6, sample M1 and M2 produced BSA solute rejection much higher than the pristine membrane (78.92%).

The incorporation of MWCNTs into the membranes improved the membrane structures, making it more hydrophilic. As for the water application process, more hydrophilic membranes were preferable so that the permeates can be filtrated easily. A study by Farahani and Vatanpour [27] reported that incorporation of nanoparticles into membrane matrix resulted in more hydrophilic surfaces which led to lower interaction and affinity between the membrane surfaces and solutes. Therefore, a higher rejection rate was achieved for nanocomposite membranes compared to the pristine membrane while the enhanced BSA rejection might be due to the lower hydrophobic interaction of BSA proteins and hydrophilic surfaces of the hybrid membranes.

These phenomenon also applied for the HA rejection as shown in Figure 7. The membrane hydrophilicity is an important key in membrane applications to determine their anti-fouling ability. Many approaches have been developed to improve membrane hydrophilicity by incorporating nanoparticles through many surface modification methods including the physical blending method. Leo et al. [40] reported that the contact angle value decreased from 70.6° to 64.5° when the SAPO-44 zeolites contents increased from 5 wt.% to 15 wt.%. In addition, the amount of HA adsorbed in membrane pores also decreased due to the enhanced membrane antifouling ability by minimizing the pore blockage that can lead to fouling. Jiang et al. [41] categorized the factors of the HA removal efficiency could be influenced by two aspects; which is the membrane average pore size and adsorption of HA on the membrane surfaces. Since the HA solute varies in sizes, the molecules which are smaller than the modified membrane can diffuse easily. Thus, the separation of HA was mainly dependent on the adsorption of HA in the membrane matrix.

Nevertheless, the cake layer which was formed on the membrane surfaces could prevent the water molecules passing through the membrane pores; causing the reduction in rejection rate. As the filtration time increased, the solutes rejection has been reduced drastically due to the thicker layer of solutes depositions on the membrane surfaces, as agreed by Guo etal. [42]. In addition, it was reported that 'over-clogging' happened because of large quantity of small macromolecules entered and filled the interstices of a cake formed by smaller-structured particles that caused a greater hydraulic resistance.

The decline in solute rejections can be correlated to membrane swelling after the membrane being exposed for long hour operation. It was observed that the membranes were swollen after the filtration process which is due to trapped water molecules and solutes molecules in the membrane pores due to the irregular size of the solutes molecules. Ibrahim et al. [15] performed a study on the permeability of PVDF/ZIF-8 membrane for pure water and domestic wastewater. The results obtained show that the permeability for both feeds was improved upon the addition of ZIF-8 nanoparticles. However, when 10 wt.% of ZIF-8 has been applied, the permeability of pure water and wastewater was reduced. This probably was due to the phenomenon of membrane swelling during the filtration process in which has reduced the affective area for permeability as previously reported by Escoda et al. [43].

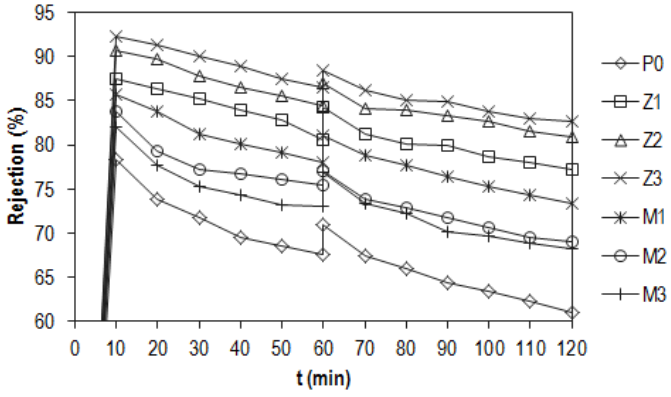

Fig. 6. Result of BSA solute rejection for PVDF membrane. Operating pressure=1bar, BSA concentration=500ppm.

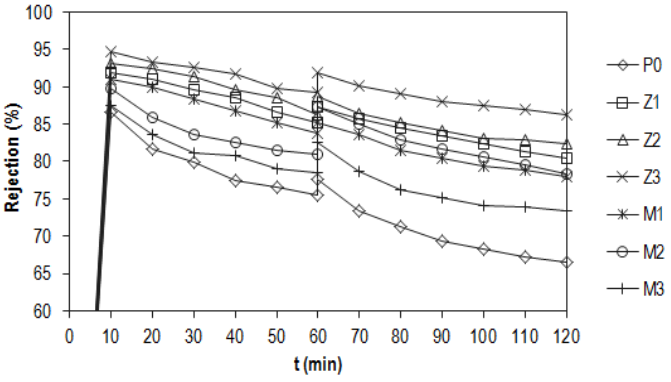

Fig. 7. Result of HA solute rejection for PVDF membrane. Operating pressure=1bar, HA concentration=500ppm.

4. Conclusions

PVDF nanocomposite membranes was successfully fabricated by introducing various compositions of MWCNT and ZIF-8 into the polymer dope. Membrane with ZIF-8 was synthesized with hexagonal-shaped with particle sizes ranging from 140 nm to 160 nm and confirmed by TEM analysis. In addition, the result of the contact angle indicated that the incorporation of nanoparticles into the membrane matrix has improved hydrophilicity behavior of PVDF membranes upon the addition of nanoparticles and PVP. In comparison, as the concentration of nanoparticles increased, the modified membranes showed an improvement in the membrane structures as the structures became more porous and spongier. For the modified membranes, the increase in nanoparticles concentration attributed to higher pure water fluxes compared to pristine. The highest water fluxes for

PVDF/ZIF-8 membranes were achieved by membrane sample Z1 with a flux value of 56.96 L/m^{2}h. Meanwhile, the highest water flux of PVDF/MWCNT membranes increased with the average of 73.03 L/m^{2}h for membrane sample M3. Furthermore, the results of the filtration test revealed that the PVDF/ZIF-8 membrane achieved highest performance of solute rejection with 0.5 wt.% concentration for HA (≥94%) and BSA (≥92%) solution as compared to other prepared membranes.

For PVDF/MWCNT membranes, M1 displayed the highest result of solute rejections for both HA solution (≥90%) and BSA (≥85%). However, all the rejection rate of the membrane samples started to decline when they are exposed to longer contact time. The FRR and flux decline rate of all prepared membranes showed a decreased in values as the filtration time increased. This indicates the potential of membrane fouling has occurred and started to deteriorate the filtration performance of the membranes. In a nutshell, the nanoparticles of ZIF-8 and MWCNTs displayed good anti-fouling properties and can be further studied for minimizing the fouling membrane. The addition of nanoparticles also improved the membrane morphologies, hydrophilicity, pure water flux and filtration performance of the modified membranes compared to pristine and it is suitable to be applied in the water separation process.

Acknowledgements

The authors gratefully acknowledge the financial support from the Ministry of Education (MOE) under FRGS Grant (FRGS/1/2019/TK05/UMP/02/17) and Universiti Malaysia Pahang (PGRS180384 Development of antibactericidal composite membrane for waste treatment and Grant RDU1901210).

References

[1] H. Basri, A.F. Ismail, M. Aziz, K. Nagai, T. Matsuura, M.S. Abdullah, B.C. Ng, Silver-filled PSF membranes for antibacterial applications - Effect of PVP and TAP addition on silver dispersion, Desalination 261(2010) 264–271. https://doi: 10.1016/j.desal.2010.05.009

[2] S. Ayyaru, Y.H. Ahn, Application of sulfonic acid group functionalized graphene oxide to improve hydrophilicity, permeability, and antifouling of PVDF nanocomposite ultrafiltration membranes, J. Membr. Sci. 525 (2017) 210–219. https://doi: 10.1016/j.memsci.2016.10.048H

[3] V. Kochkodan, N. Hilal, Comprehensive review on surface modified polymer membranes for biofouling mitigation, Desalination 356 (2015) 187-207. https://doi: 10.1016/j.desal.2014.09.015

[4] D. Rana, T. Matsuura, Surface modifications for antifouling membranes, Chem. Rev. 110(4) (2010) 2448-2471. https://doi: 10.1021/cr800208y

[5] V. Vatanpour, A. Shockravi, H. Zarrabi, Z. Nikjavan, A. Javadi, Fabrication and characterization of anti-fouling and anti-bacterial ag-loaded graphene oxide/polyethersulfone mixed matrix membrane. J. Ind. Eng. Chem. 30 (2015) 342–352. https://doi: 10.1016/j.jiec.2015.06.004

[6] P. Dallas, V.K. Sharma, R. Zboril, Silver polymeric nanocomposites as advanced antimicrobial agents: Classification, synthetic paths, applications, and perspectives, Adv. Colloid Inter. Sci. 166 (2011) 119–135. https://doi: 10.1016/j.cis.2011.05.008

[7] A. Munoz-Bonilla, M. Fernandez–Garcia, Polymeric materials with antimicrobial activity, Prog. Polym. Sci. 37 (2) (2012) 281-339. https://doi.org/10.1016/j.progpolymsci.2011.08.005

[8] Z. Lai, G. Bonilla, I. Diaz, J.G. Nery, K. Sujaoti, M.A. Amat, E. Kokkoli, O.Terasaki, R.W. Thompson, M. Tsapatsis, D.G. Vlachos, Microstructural optimization of a zeolite membrane for organic vapor separation, Science 300 (5618) (2003) 456–460. https://doi: 10.1126/science.1082169

[9] Y. Zhao, Z. Xu, M. Shan, C. Min, B. Zhou, Y. Li, B. Li, L. Liu, X. Qian, Effect of graphite oxide and multi-walled carbon nanotubes on the microstructure and performance of PVDF membranes, Sep. Purif. Technol. 103 (2013) 78–83. https://doi: 10.1016/j.seppur.2012.10

[10] N.A.H.M. Nordin, A.F. Ismail, Y. Noorhana, Zeolitic imidazole framework 8 decorated graphene oxide (ZIF-8/GO) mixed-matrix membrane (MMM) for CO_2/CH_4 separation, J. Teknologi 79 (2017) 59-63. https://doi: 10.11113/jt.v79.10438

[11] L.X. Dong, H.W. Yang, S.T. Liu, X. M. Wang, Y.F. Xie, Fabrication and anti-biofouling properties of alumina and zeolite nanoparticle embedded ultrafiltration membranes, Desalination 365 (2013) 70–78. https://doi: 10.1016/j.desal.2015.02.023

[12] N. A. H. M. Nordin, A.F. Ismail, N. Misdan, N.A.M. Nazri, Modified ZIF-8 mixed matrix membrane for CO_2/CH_4 separation. AIP Conf. Proc. 1891 (2017) 020091. https://doi: 10.1063/1.5005424

[13] A. Alpatova, E-S. Kim, X. Sun, G. Hwang, Y. Liu, M.G. El-Din, Fabrication of porous polymeric nanocomposite membranes with enhanced antifouling properties: effect of casting composition, J. Membr. Sci. 444 (2013) 449–460. https://doi: 10.1016/j.memsci.2013.05.034

[14] A. Bottino, G. Capannelli, A. Comite, Preparation and characterization of novel porous PVDF–ZrO_2 composite membranes, Desalination, 146(1-3) (2002) 35–40. https://doi: 10.1016/S0011-9164(02)00469-1

[15] N.A. Ibrahim, M.D.H. Wirzal, N.A.H. Nordin, N. S. Halim, Development of polyvinylidene fluoride (PVDF)-ZIF8 membrane for wastewater treatment, IOP Conf. Ser.: Earth Environ. Sci.140 (2018) 12-21. https://doi :10.1088/1755-1315/140/1/012021

[16] J.S. Taurozzi, H. Arul, V.Z. Bosak, A.F. Burban, T.C. Voice, M.L. Bruening, V.V. Tarabaraa, Effect of filler incorporation route on the properties of poly-sulfone-silver nanocomposite membranesof different porosities, J. Membr. Sci. 325 (2008) 58-68. https://doi: 10.1016/j.memsci.2008.07.010

[17] B. Hudaib, V. Gomes, J. Shi, C. Zhou, Z. Liu, Poly(vinylidene fluoride)/polyaniline/MWCNT nanocomposite ultrafiltration membrane for natural organic matter removal, Sep. Purif. Technol. 190 (2018) 143-155. https://doi: 10.1016//j.seppur.2017.08.026

[18] Z. Yu, G. Zeng, Y. Pan, L. Lv, H. Min, L. Zhang, Y. He, Effect of functionalized multi-walled carbon nanotubes on the microstructure and performances of PVDF membranes, RSC Adv. 5 (2015) 75998-76006. https://10.1039/C5RA12819F

[19] R. Naim, A.F. Ismail, A. Mansourizadeh, Effect of non-solvent additives on the structure and performance of PVDF hollow fiber membrane contactor for CO_2 stripping, J. membr. Sci. 423–424 (2012) 503–513. https://doi: 10.1016/j.memsci.2012.08.052

[20] I.C. Kim, K.H. Lee, T.M. Tak, Preparation and characterization of integrally skinned uncharged polyetherimide asymmetric nanofiltration membrane, J. Membr. Sci. 183 (2) (2001) 235–247. https://doi: 10.1016/S0376-7388(00)00588-3

[21] I.H. Aljundi, Desalination characteristics of TFN/RO membrane incorporated with ZIF-8 nanoparticles, Desalination 420 (2017) 12-20. https://doi: 10.1016/j.desal.2017.06.020

[23] H. Duan, D. Wang, Y. Li, Green chemistry for nanoparticle synthesis, Chem. Soc. Rev. 44 (16) (2015) 5778-5792. https://doi:10.1039/c4cs00363b

[24] Y. Zhao, Z. Xu, M. Shan, C. Min, B. Zhou, Y. Li, B. Li, L. Liu, X. Qian, Effect of graphite oxide and multi-walled carbon nanotubes on the microstructure and performance of PVDF membranes, Sep. Purif. Technol. 103 (2013) 78-83. https://doi: 10.1016/j.seppur.2012.10.012

[25] A. Rahimpour, M. Jahanshahi, B. Rajaeian, M. Rahimnejad, TiO_2 entrapped nano-composite PVDF/SPES membranes: Preparation, characterization, antifouling and antibacterial properties, Desalination 278 (2011) 343–353. https://doi: 10.1016/j.desal.2011.05.049

[26] J. Xu, Z.L. Xu, Poly(vinyl chloride) (PVC) Hollow fiber ultrafiltration membranes prepared from PVC/additives/solvent, J. Membr. Sci. 208 (2002) 203–212. https://doi: S0376-7388(02)00261-2

[27] M.H.D.A. Farahani, V. Vatanpour, A comprehensive study on the performance and antifouling enhancement of the PVDF mixed matrix membranes by embedding different nanoparticulates: clay, functionalized carbon nanotube, SiO_2 and TiO_2, Sep. Purif. Technol. 197 (2018) 372-381. https://doi: 10.1016/j.seppur.2018.01.031

[28] J. Yin, G. Zhu, B. Deng, Multi-walled carbon nanotubes (MWCNTs)/polysulfone (PSU) mixed matrix hollow fiber membranes for enhanced water treatment, J. Membr. Sci. 437 (2013) 237–248. https://doi: 10.1016/j.memsci.2013.03.021

[29] J. Meng, L. Song, H.Y. Xu, H. Kong, C.Y. Wang, X.T. Guo, S. Xie, Effects of single-walled carbon nanotubes on the functions of plasma proteins and potentials in vascular prostheses, Nanomedicine 1(2) (2005) 1136–142. https://doi:10.1016/j.nano.2005.03.003

[30] P.S. Goh, B.C Ng, W.J. Lau, A.F. Ismail, Inorganic nanomaterials in polymeric ultrafiltration membranes for water treatment, Sep. Purif. Rev. 44 (3) (2015) 216-249. https://doi: 10.1080/15422119.2014.926274

[31] C-Y. Tang, W. Chen, W-Q. Chen, Q. Fu, Z-L. Q, Y. Ye, M. Onishi, N. Abe, Effect of solution extrusio rate on morphology and performance of polyvinylidene fluoride hollow fiber membranes usingpolyvinyl pyrrolidone as an additive, Chin. J. Polym. Sci. 28 (4) (2010) 527-533. https://doi: 10.1007/s10118-010-9054-5

[32] E. Arkhangelsky, A. Duek, V. Gitis, Maximal pore size in UF membranes, J. Membr. Sci. 394–395 (2012) 89–97. https://doi: 10.1016/j.memsci.2011.12.031

[33] C.H. Hu, C.H. Liu, L.Z. Chen., Y.C. Peng., S.S. Fan, Resistance-pressure sensitivity and a mechanism study of multiwall carbon nanotube networks/poly (dimethylsiloxane) composites. Appl. Phys. Lett. 93 (3) (2008), 033-108. https://doi: 10.1063/1.2961028

[34] P. Marel, W. Meer, Influence of membrane properties on fouling in submerged membrane bioreactors, J. Membr. Sci 348 (1-2) (2010), 66-74. https://doi:10.1016/j.memsci.2009.10.054

[35] M.T. Khan, S. Takizawa, Z. Lewandowski, W.L. Jones, A.K. Camper, H. Katayama, F. Kurisu, S. Ohgaki, Membrane fouling due to dynamic particle size changes in the aerated hybrid PAC-MF system, J. Membr. Sci. 371 (1-2) (2011) 99-107. https://doi: 10.1016/j.memsci.2011.01.017

[36] V-L. Turcaud, M-R. Wienser, J-Y. Bottero, Fouling in tangential-flow ultrafiltration: The effect of colloid size and coagulation pretreatment, J. Membr. Sci. 52 (2) (1990) 173-190. https://doi: 10.1016/S0376-7388(00)80484-6

[37] M. Hashino, K. Hirami, T. Ishigami, Y. Ohmukai, T. Maruyama, N. Kubota, H. Matsuyama, Effect of kinds of membrane materials on membrane fouling with BSA, J. Membr. Sci. 384 (2011) 1-2, 157-165.https://doi: 10.1016/j.memsci.2011.09.015

[38] Q. Zhao, J. Hou, J. Shen, J. Liu, Y. Yatao Zhang, Long-lasting antibacterial behavior of a novel mixed matrix water purification membrane. J. Mater. Chem. A. 3 (2015), 18696–18705. https://doi: 10.1039/c5ta06013c

[39] A. Alpatova, M. Meshref, K.N. McPhedran, M.G. El-Din, M. G., Composite

polyvinylidene fluoride (PVDF) membrane impregnated with Fe_2O_3 nanoparticles and multiwalled carbon nanotubes for catalytic degradation of organic contaminants, J. Membr. Sci. 490 (2015), 227–235. https://doi: 10.1016/j.memsci.2015.05.001

[40] C.P. Leo, N.H. Ahmad Kamil, M.U.M Junaidi, S.N.M Kamal, A.L. Ahmad, The potential of SAPO-44 zeolite filler in fouling mitigation of polysulfone ultrafiltration membrane, Sep. Purif. Technol. 103 (2013), 84–91. https://doi:10.1016/j.seppur.2012.10.019

[41] T. Jiang, M.D. Kennedy, V.D. Schepper, S.N., Nam, I. Nopens, P.A. Vanrollegham, G. Amy, Characterization of soluble microbial products and their fouling impacts in membrane bioreactors. Envi. Sci. Technol. 44 (17) (2010), 6642-6648. https://doi.org/10.1021/es100442g

[42] H. Guo, Y. Wyart, J. Perot, F. Nauleau, P. Moulin, Low-pressure membrane integrity tests for drinking water treatment, Water Res. 44 (2010), 41-57. https://doi: 10.1016/j.watres.2009.09.032

[43] A. Escoda, P. Fievet, S. Lakard, A. Szymczyk, S. Deon, Influence of salts on the rejection of polyethyleneglycol by an NF organic membrane: Pore swelling and salting-out effects. J. Membr. Sci. 347 (1-2), (2010) 174-182. https://doi.org/10.1016/j.memsci.2009.10.021